

Article

On K -Banhatti, Revan Indices and Entropy Measures of $MgO(111)$ Nanosheets via Linear Regression

Norah Almalki ¹ and Hafsah Tabassum ^{2,3,*} 

¹ Department of Mathematics and Statistics, College of Science, Taif University, Al Hawiyah 21944, Saudi Arabia; norah@tu.edu.sa

² Department of Mathematics, Faculty of Science, King Mongkut's University of Technology Thonburi, Bangkok 10140, Thailand

³ Mathematics and Statistics with Applications (MaSA), Faculty of Science, King Mongkut's University of Technology Thonburi, Bangkok 10140, Thailand

* Correspondence: hafsah.tabassum@mail.kmutt.ac.th

Abstract: The structure and topology of chemical compounds can be determined using chemical graph theory. Using topological indices, we may uncover much about connectivity, complexity, and other important aspects of molecules. Numerous research investigations have been conducted on the K -Banhatti indices and entropy measurements in various fields, including the study of natural polymers, nanotubes, and catalysts. At the same time, the Shannon entropy of a graph is widely used in network science. It is employed in evaluating several networks, including social networks, neural networks, and transportation systems. The Shannon entropy enables the analysis of a network's topology and structure, facilitating the identification of significant nodes or structures that substantially impact network operation and stability. In the past decade, there has been a considerable focus on investigating a range of nanostructures, such as nanosheets and nanoparticles, in both experimental and theoretical domains. As a very effective catalyst and inert substrate, the MgO nanostructure has received a lot of interest. The primary objective of this research is to study different indices and employ them to look at entropy measures of magnesium oxide(111) nanosheets over a wide range of p values, including $p = 1, 2, 3, \dots, j$. Additionally, we conducted a linear regression analysis to establish the correlation between indices and entropies.

Keywords: K -Banhatti indices; magnesium oxide(111); topological indices

MSC: 05C92



Citation: Almalki, N.; Tabassum, H. On K -Banhatti, Revan Indices and Entropy Measures of $MgO(111)$ Nanosheets via Linear Regression. *Mathematics* **2024**, *12*, 561. <https://doi.org/10.3390/math12040561>

Academic Editors: Hilal Ahmad, Yilun Shang and Andrea Scozzari

Received: 30 November 2023

Revised: 7 February 2024

Accepted: 9 February 2024

Published: 13 February 2024



Copyright: © 2024 by the authors. Licensee MDPI, Basel, Switzerland. This article is an open access article distributed under the terms and conditions of the Creative Commons Attribution (CC BY) license (<https://creativecommons.org/licenses/by/4.0/>).

1. Introduction

Chemical graph theory facilitates establishing a connection between the graphical and chemical structure of molecules through quantitative structure-property relationships and quantitative structure-activity relationships [1–3]. Due to the extensive production growth in the chemical industry, the importance of chemical graph theory has increased. Consequently, it is important to thoroughly analyze the chemical properties of these novel medications and chemicals to utilize them effectively. A lot of research has been carried out to determine how chemical properties like molecular structure, toxicity, melting point, and freezing point are related [4,5].

The main goal of “quantitative structure-property relationships” and “quantitative structure-activity relationships” is to examine the connections between molecular structures and the properties or activities they have in different areas like medicine, pharmaceuticals, medical research, rational drug design, and experimental science [6]. The researchers analyzed different behaviors of chemical compounds in quantitative structure-property relationships [7,8] through topological indices. Kirmani et al. [9] examined the different topological variants and the physicochemical attributes of drugs employed in treating

coronavirus. Hosseini and colleagues classify the degree-based indices according to their predictive capacity [10]. The study conducted by Hosseini and Shafiei [10] investigated the correlation between several chemical indices and thermodynamic properties.

The K -Banhatti indices and entropy measures are also very well-known indices to study molecular graphs of compounds. These indices have been applied to analyze the topological characteristics of natural polymers, such as cellulose networks [11]. Ghani et al. looked into the entropies and K -Banhatti indices of C_6H_6 in various chemical networks [12]. The main goal of their study was to find out how the K -Banhatti indices work with other molecules. V. R. Kulli developed the modified K -Banhatti indices [13,14]. Chaluvvaraju came up with the Zagreb version of the K -Banhatti index of a graph, which has been used to study the topological properties of graphs [15]. Kiran Naz et al. studied the polycyclic random chains and computed their multiplicative and hyper K multiplicative K Bhanhatti indices [16]. The types of polycyclic chains that they studied include polyphenyl and spiro chains. Hussain et al. [17] studied k Bhanhatti indices and entropy measures of rhodium (III) chloride. Using the line-fit method, they conducted their research using linear regression analysis and established the relationship between indices and entropy. Ref. [18] calculated the M -polynomial of C_3 and H_6 nanosheets and computed some topological indices by using M -polynomials. Ref. [12] calculated the precise values of K -Banhatti Indices of C_6H_6 by using atom-bond partitioning method based on valencies K -Banhatti indices provide valuable information about the connectivity and complexity of graph structures. In the context of $MgO(111)$, understanding the topological properties of its molecular graph is essential for predicting its behavior.

Along with studying the topological indices, researchers studied the entropy of these indices to thoroughly study the behavior of molecules. The computation of indices and entropy measures provides valuable insights into the structural and topological characteristics of polymers. Entropy is a fundamental concept in various fields such as information theory, thermodynamics, and statistical mechanics, and is important in understanding the behavior and characteristics of systems. Mansoor et al. [11] looked into determining molecular descriptors along with entropy measures for isomeric natural polymers. Shannon introduced the concept of entropy to quantify a system's randomness and information content. The mathematical formula of Shannon entropy is given as under:

$$E_{\phi}(M) = \sum_{xy \in W(M)} \frac{\phi(xy)}{\sum_{xy \in W(M)} \phi(xy)} \log \left[\frac{\phi(xy)}{\sum_{xy \in W(M)} \phi(xy)} \right] \quad (1)$$

Metal oxides are a significant category of materials with an extensive range of features, including insulating, semiconducting, and conducting characteristics. These materials have been utilized in several fields, including technological devices, personal care products, and catalysts. One case is the typical rock salt configuration of bulk MgO (magnesium oxide), which serves various purposes. MgO is a diamagnetic oxide with ionic properties, exhibiting insulating behavior. It possesses a significant band gap of 7.8 eV; this material is inert and has an extremely high melting point.

Additionally, it accelerates chemical reactions and offers a suitable base for various chemicals, including group III-V elements, metals, and high-pressure superconductors. Because of its non-toxic and ecologically favorable properties, it is extensively employed as a sorbent for eliminating dyes and metallic substances. It can also be utilized as an optical material and constituent of optical composites [19,20]. In the past decade, there has been a significant focus on investigating a range of nanostructures, such as nanosheets, nanowires, nano-belts, and nanoparticles, in both experimental and theoretical domains [19,21,22]. As of now, the effective synthesis of MgO thin films with two distinct facets, namely (111) and (100), has been achieved. As a very effective catalyst and inert substrate, the MgO nanostructure received a lot of interest [23]. Magnesium oxide nanosheets, which have a band gap between 2.75 and 4.38 eV, could be very useful in UV-electronic devices on the nanoscale level.

Understanding MgO(111)’s structural and topological properties is crucial for predicting its behavior and optimizing its performance in different applications. By representing the crystal structure of Magnesium oxide as a graph, it is possible to analyze its connectivity, complexity, and other topological characteristics. Topological indices of MgO(111) can be used to quantify its structural features and predict its properties [24]. This study aims to investigate the characteristics of magnesium oxide(111) nanosheets across a range of p values, encompassing $p = 1, 2, 3, \dots, j$.

2. Preliminaries and Mathematical Framework

Chemical graph theory involves the representation of a molecule as a graph, where the atoms are denoted as vertices, and the bond between atoms is represented by as an edge. The graph M is an improvised representation of a magnesium oxide (111) nanosheet molecule. The symbol X denotes the vertex set, whereas W is the edge set representing the atoms and the bond between them, respectively. The cardinality of X in a graph is commonly referred to as the order, whereas the total edges represent the size of the graph. The chemical networks consist of nodes, represented by x and y , and are connected by edges labeled as $w = xy$. The vertex x degree is represented by $d(x)$ and indicates the total edges connected to that vertex. Recently, an innovative concept of the edge degree has been introduced, denoted as $d(e) = d(x) + d(y) - 2$. The maximum degree of the graph can be represented by $\Delta(M)$ and $\delta(M)$, $\kappa(x) = \Delta(M) + \delta(M) - d(x)$ and $r(\bar{x}) = \Delta(M) + \delta(M) - d(x)$. Table 1 contains the formulas of all the indices under consideration.

Table 1. Topological Indices.

Indices	Notations-	Formula
The first K -Banhatti Index [14]	$B_1(M)$ -	$\sum_{xw} [d(x) + d(e)]$
The second K -Banhatti Index [14]	$B_2(M)$ -	$\sum_{xw} [d(x) \cdot d(e)]$
The first K hyper-Banhatti Index [25]	$HB_1(M)$ -	$\sum_{xw} [d(x) + d(e)]^2$
The second K hyper-Banhatti Index [25]	$HB_2(M)$ -	$\sum_{xw} [d(x) \cdot d(e)]^2$
The K -Banhatti harmonic Index [26]	$H_b(M)$ -	$\sum_{xw} [\frac{2}{d(x)+d(e)}]$
The first hyper Revan Index [25]	$\eta R_1(M)$ -	$\sum_{w=xy} [\kappa(x) + \kappa(y)]^2$
The second hyper Revan Index [25]	$\eta R_2(M)$ -	$\sum_{w=xy} [\kappa(x) \cdot \kappa(y)]^2$
The third Revan Index [26]	$\eta R_3(M)$ -	$\sum_{w=xy} [\kappa(x) - \kappa(y)]$
The first Revan vertex Index [26]	$R_1(M)$ -	$\sum_{w=xy} [\kappa(\bar{x})]^2$

Various methodologies are employed to calculate the results, including vertex and edge division and combinatorial techniques. The indices associated with degrees are computed manually utilizing a simple calculator, and the results’ reliability is validated using Python. The chemical structures of magnesium oxide are constructed using Chem-Draw. The molecular graph of magnesium oxide (111) is given in Figure 1.

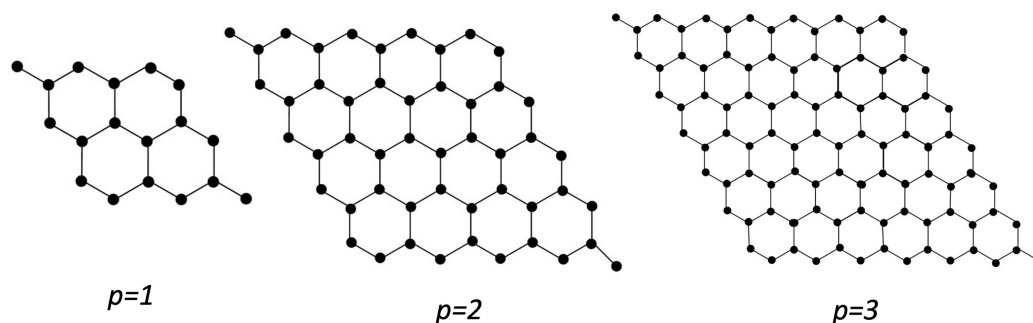


Figure 1. Molecular Graph of MgO(111).

The Magnesium Oxide $MgO(111)$ nanosheet has order $2(4p^2 + 4p + 1)$ and size $12p^2 + 8p + 1$. The vertex set is divided into three categories (or subsets) X_1, X_2, X_3 depending upon their degrees given in Table 2.

Table 2. Vertex Division of $MgO(111)$.

$d(x)$	Cardinality-	$r(\bar{x})$
X_1	2-	3
X_2	$8p-$	2
X_3	$8p^2-$	1

The edge set of $MgO(111)$ has 4 categories W_1, W_2, W_3, W_4 depending upon the degrees of their end vertices that are given in Table 3. W_1 has two edges where $d(x) = 1$ and $d(y) = 3$. W_2 has two edges where $d(x) = 2 = d(y)$. W_3 with $d(x) = 2$ and $d(y) = 3$ contains $4(4p - 1)$ edges. W_4 contains $4p(3p - 2) + 1$ edges where $d(x) = d(y) = 3$.

Table 3. Edge Division of $MgO(111)$.

Edges	$(d(x), d(y))$	Frequency	$d(e)$	$\kappa(x)$	$\kappa(y)$
W_1	(1,3)	2	2	3	1
W_2	(2,2)	2	2	2	2
W_3	(2,3)	$4(4p - 1)$	3	2	1
W_4	(3,3)	$4p(3p - 2) + 1$	4	1	1

3. Results and Discussion

We computed the K -Banhatti and Revan indices using multiple approaches, such as vertex degree analysis and edge partitioning. Following that, we calculated entropy utilizing these indices. Python has been used for result validation and correlation analysis. By employing the data shown in Tables 3 and 4, we can compute K -Banhatti indices, as given below.

- The first K -Banhatti Index

$$\begin{aligned}
 \mathcal{B}_1(M) &= \sum_{xw} [d(x) + d(e)] \\
 &= 2[(1 + 2) + (3 + 2)] + 2[(2 + 2) + (2 + 2)] + 4(4p - 1) \\
 &\quad [(2 + 3) + (3 + 3)] + (4p(3p - 2) + 1)[(3 + 4) + (3 + 4)] \\
 &= 32 + 44(4p - 1) + 56p(3p - 2) + 14 \\
 &= 168p^2 + 64p + 2
 \end{aligned}$$

- The second K -Banhatti Index

$$\begin{aligned}
 \mathcal{B}_2(M) &= \sum_{xw} [d(x) \times d(e)] \\
 &= 2[(1 \times 2) + (3 \times 2)] + 2[(2 \times 2) + (2 \times 2)] + 4(4p - 1) \\
 &\quad [(2 \times 3) + (3 \times 3)] + (4p(3p - 2) + 1)[(3 \times 4) + (3 \times 4)] \\
 &= 32 + 32 + 15(16p - 4) + 46p(3p - 2) + 96 \\
 &= 288p^2 + 48p + 68
 \end{aligned}$$

- The first hyper K -Banhatti Index

$$\begin{aligned} \mathcal{HB}_1(M) &= \sum_{xw} [d(x) + d(e)]^2 \\ &= 2[(1 + 2)^2 + (3 + 2)^2] + 2[(2 + 2)^2 + (2 + 2)^2] + 4(4p - 1) \\ &\quad [(2 + 3)^2 + (3 + 3)^2] + (4p(3p - 2) + 1)[(3 + 4)^2 + (3 + 4)^2] \\ &= 132 + 244(4p - 1) + 98[4p(3p - 2) + 1] \\ &= 1176p^2 + 192p - 14 \end{aligned}$$

- The second hyper K -Banhatti Index

$$\begin{aligned} \mathcal{HB}_2(M) &= \sum_{xw} [d(x) \times d(e)]^2 \\ &= 2[(1 \times 2)^2 + (3 \times 2)^2] + 2[(2 \times 2)^2 + (2 \times 2)^2] + 4(4p - 1) \\ &\quad [(2 \times 3)^2 + (3 \times 3)^2] + (4p(3p - 2) + 1)[(3 \times 4)^2 + (3 \times 4)^2] \\ &= 74 + 468(4p - 1) + 288[4p(3p - 2) + 1] \\ &= 3456p^2 - 432p - 36 \end{aligned}$$

- The K -Banhatti harmonic Index

$$\begin{aligned} \mathcal{H}_b(M) &= \sum_{xw} \left[\frac{2}{d(x) + d(e)} \right] \\ &= 2 \left[\frac{2}{(1 + 2)} + \frac{2}{(3 + 2)} \right] + 2 \left[\frac{2}{(2 + 2)} + \frac{2}{(2 + 2)} \right] + 4(4p - 1) \\ &\quad \left[\frac{2}{(2 + 3)} + \frac{2}{(3 + 3)} \right] + (4p(3p - 2) + 1) \left[\frac{2}{(3 + 4)} + \frac{2}{(3 + 4)} \right] \\ &= \frac{62}{15} + \frac{44}{15}(4p - 1) + \frac{p}{7}(3p - 2) + \frac{4}{7} \\ &= \frac{48p^2}{7} + \frac{752p}{105} + \frac{62}{35} \end{aligned}$$

- The first hyper Revan Index

$$\begin{aligned} \eta R_1(M) &= \sum_{w=xy} [\kappa(x) + \kappa(y)]^2 \\ &= 2(3 + 1)^2 + 2(2 + 2)^2 + 4(4p - 1)(2 + 1)^2 \\ &\quad + [4p(3p - 2) + 1](1 + 1)^2 \\ &= 32 + 32 + 36(4p - 1) + 4[4p(3p - 2) + 1] \\ &= 48p^2 + 112p + 32 \end{aligned}$$

- The second hyper Revan Index

$$\begin{aligned} \eta R_2(M) &= \sum_{w=xy} [\kappa(x) \times \kappa(y)]^2 \\ &= 2(3)^2 + 2(2 \times 2)^2 + 4(4p - 1)(2 \times 1)^2 \\ &\quad + [4p(3p - 2) + 1](1 \times 1)^2 \\ &= 18 + 32 + 16(4p - 1) + [4p(3p - 2) + 1] \\ &= 12p^2 + 56p + 35 \end{aligned}$$

- The third Revan Index

$$\begin{aligned} \eta R_3(M) &= \sum_{w=xy} [\kappa(x) - \kappa(y)] \\ &= 2(3 - 1) + 2(2 - 2) + 4(4p - 1)(2 - 1) \\ &\quad + [4p(3p - 2) + 1](1 - 1) \\ &= 16p \end{aligned}$$

- The first Revan Vertex Index

$$\begin{aligned} \mathcal{R}_1(M) &= \sum_{w=xy} [r(\bar{x})]^2 \\ &= 2(3)^2 + 8p(2)^2 + 8p^2(1)^2 \\ &= 8p^2 + 32p + 18 \end{aligned}$$

Upon assessing Table 4 and Figure 2, it becomes clear that the expansion rate of the $\mathcal{B}_1(M)$ index is significantly higher than that of the $\mathcal{B}_2(M)$ index as p increases. Moreover, it is noticeable that when the value of p increases, the growth rate of the $\mathcal{HB}_2(M)$ index surpasses that of $\mathcal{HB}_1(M)$. Moving on, it can be observed that as p increases, the $\mathcal{R}_1(M)$ index grows far faster than $\mathcal{H}_b(M)$. Similarly, the $\eta R_1(M)$ index grows faster than the $\eta R_2(M)$ and $\eta R_3(M)$ indices as p increases. $\eta R_3(M)$ shows a very steady increase.

Table 4. K-Banhatti and Revan indices of MgO(111).

p	$\mathcal{B}_1(M)$	$\mathcal{B}_2(M)$	$\mathcal{HB}_1(M)$	$\mathcal{HB}_2(M)$	$\mathcal{H}_b(M)$	$\eta R_1(M)$	$\eta R_2(M)$	$\eta R_3(M)$	$\mathcal{R}_1(M)$
1	234	404	1354	2988	15.790	192	103	16	58
2	802	1316	5074	12,924	43.523	448	195	32	114
3	1706	2804	11,146	29,772	84.971	800	311	48	186
4	2946	4868	19,570	53,532	140.133	1248	451	64	274
5	4522	7508	30,346	84,204	209.00	1792	615	80	378
6	6434	10,724	43,474	121,788	291.6	2432	803	96	498
7	8682	14,516	58,954	166,284	387.90	3168	1015	112	634
8	11,266	18,884	76,786	217,692	497.92	4000	1251	128	786
9	14,186	23,828	96,970	276,012	621.65	4928	1511	144	954
10	17,442	29,348	119,506	341,244	759.10	5952	1795	160	1138

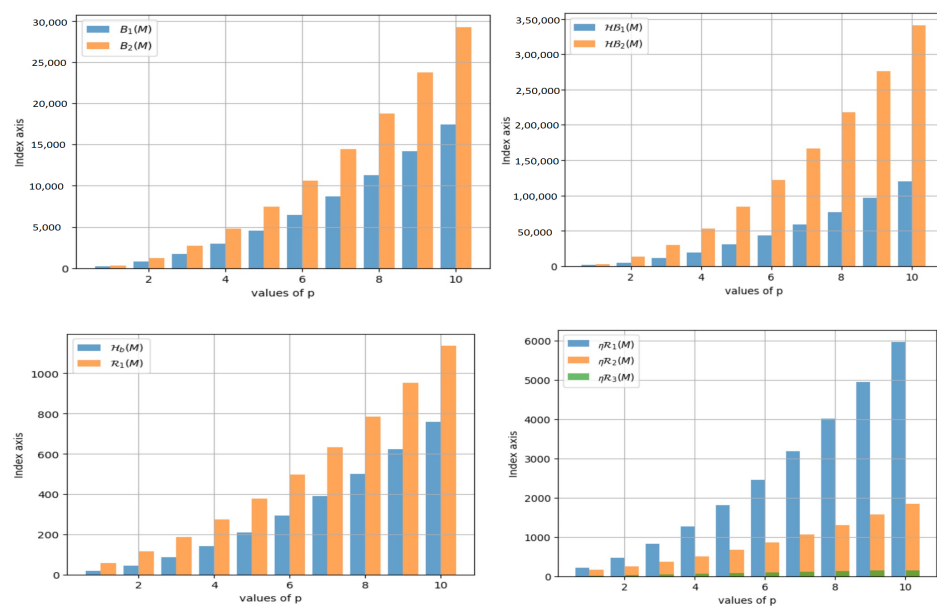


Figure 2. Graphical Representation of K-Banhatti and Revan Indices.

4. K-Banhatti Entropy and Linear Regression Analysis

In this section, the results of the entropy of the indices are given, along with the discussion on corresponding numerical outcomes. In addition, we include visualizations of topological indices for different parameter values. The following entropy values are found using the above-estimated indices and the values from Table 3 in Equation (1).

- The first K-Banhatti entropy

$$\mathcal{E}_{\mathcal{B}_1} = \log(\mathcal{B}_1) - \frac{1}{\mathcal{B}_1} \log\left[\prod_{xy \in W(M)} (d(x) + d(e))^{(d(x)+d(e))}\right]$$

$$\mathcal{E}_{\mathcal{B}_1} = \log(168p^2 + 64p + 2) - \frac{\log(2 \times (8)^8)}{168p^2 + 64p + 2} - \frac{\log(2 \times (8)^8)}{168p^2 + 64p + 2}$$

$$- \frac{\log(4(4p - 1) \times (11)^{11})}{168p^2 + 64p + 2} - \frac{\log((4p(3p - 2) + 1) \times (14)^{14})}{168p^2 + 64p + 2}$$

- The second K-Banhatti entropy

$$\mathcal{E}_{\mathcal{B}_2} = \log(\mathcal{B}_2) - \frac{1}{\mathcal{B}_2} \log\left[\prod_{xy \in W(M)} (d(x) \times d(e))^{(d(x) \times d(e))}\right]$$

$$\mathcal{E}_{\mathcal{B}_2} = \log(288p^2 + 48p + 68) - \frac{\log(2 \times (8)^8)}{288p^2 + 48p + 68} - \frac{\log(2 \times (8)^8)}{288p^2 + 48p + 68}$$

$$- \frac{\log(4(4p - 1) \times (15)^{15})}{288p^2 + 48p + 68} - \frac{\log((4p(3p - 2) + 1) \times (24)^{24})}{288p^2 + 48p + 68}$$

- The first hyper K-Banhatti entropy

$$\mathcal{E}_{\mathcal{HB}_1(M)} = \log(\mathcal{HB}_1(M)) - \frac{1}{\mathcal{HB}_1(M)}$$

$$\log\left[\prod_{xy \in W(M)} ((d(x) + d(e))^2)^{(d(x)+d(e))^2}\right]$$

$$\mathcal{E}_{\mathcal{HB}_1(M)} = \log(1176p^2 + 192p - 14) - \frac{\log(2 \times (34)^{34})}{1176p^2 + 192p - 14}$$

$$- \frac{\log(2 \times (32)^{32})}{1176p^2 + 192p - 14} - \frac{\log(4(4p - 1) \times (61)^{16})}{1176p^2 + 192p - 14}$$

$$- \frac{\log((4p(3p - 2) + 1)(98)^{98})}{1176p^2 + 192p - 14}$$

- The second hyper K-Banhatti entropy

$$\mathcal{E}_{\mathcal{HB}_2(M)} = \log(\mathcal{HB}_2(M)) - \frac{1}{\mathcal{HB}_2(M)}$$

$$\log\left[\prod_{xy \in W(M)} ((d(x) \times d(e))^2)^{(d(x) \times d(e))^2}\right]$$

$$\mathcal{E}_{\mathcal{HB}_2(M)} = \log(3456p^2 - 432p - 36) - \frac{\log(2 \times (40)^{40})}{3456p^2 - 432p - 36}$$

$$- \frac{\log(2 \times (32)^{32})}{3456p^2 - 432p - 36} - \frac{\log(4(4p - 1) \times (117)^{117})}{3456p^2 - 432p - 36}$$

$$- \frac{\log((4p(3p - 2) + 1) \times (288)^{288})}{3456p^2 - 432p - 36}$$

- The *K*-Banhatti harmonic entropy

$$\begin{aligned} \mathcal{E}_{\mathcal{H}_b(M)} &= \log(\mathcal{H}_b(M)) - \frac{1}{\mathcal{H}_b(M)} \\ &\quad \log\left[\prod_{xy \in W(M)} \left(\frac{2}{d(x) + d(y)}\right)^{\binom{2}{d(x)+d(y)}}\right] \\ \mathcal{E}_{\mathcal{H}_b(M)} &= \log(6.857p^2 + 7.162p + 1.77) - \frac{\log(2 \times (\frac{16}{15})^{\frac{16}{15}})}{6.857p^2 + 7.162p + 1.77} \\ &\quad - \frac{\log(2 \times (1)^1)}{6.857p^2 + 7.162p + 1.77} - \frac{\log(4(4p - 1) \times (\frac{11}{15})^{\frac{11}{15}})}{6.857p^2 + 7.162p + 1.77} \\ &\quad - \frac{\log((4p(3p - 2) + 1) \times (\frac{4}{7})^{\frac{4}{7}})}{6.857p^2 + 7.162p + 1.77} \end{aligned}$$

- The first hyper Revan entropy

$$\begin{aligned} \mathcal{E}_{\eta R_1(M)} &= \log(\eta R_1(M)) - \frac{1}{\eta R_1(M)} \\ &\quad \log\left[\prod_{xy \in W(M)} ((\kappa(x) + \kappa(y))^2)^{(\kappa(x) + \kappa(y))^2}\right] \\ \mathcal{E}_{\eta R_1(M)} &= \log(48p^2 + 112p + 32) - \frac{\log(2 \times (16)^{16})}{48p^2 + 112p + 32} \\ &\quad - \frac{\log(2 \times (16)^{16})}{48p^2 + 112p + 32} - \frac{\log(4(4p - 1) \times (9)^9)}{48p^2 + 112p + 32} \\ &\quad - \frac{\log((4p(3p - 2) + 1) \times (4)^4)}{48p^2 + 112p + 32} \end{aligned}$$

- The second hyper Revan entropy

$$\begin{aligned} \mathcal{E}_{\eta R_2(M)} &= \log(\eta R_2(M)) - \frac{1}{\eta R_2(M)} \\ &\quad \log\left[\prod_{xy \in W(M)} ((\kappa(x) \times \kappa(y))^2)^{(\kappa(x) \times \kappa(y))^2}\right] \\ \mathcal{E}_{\eta R_2(M)} &= \log(12p^2 + 56p + 35) - \frac{\log(2 \times (9)^9)}{12p^2 + 56p + 35} \\ &\quad - \frac{\log(2 \times (16)^{16})}{12p^2 + 56p + 35} - \frac{\log(4(4p - 1) \times (4)^4)}{12p^2 + 56p + 35} \\ &\quad - \frac{\log((4p(3p - 2) + 1)(1)^1)}{12p^2 + 56p + 35} \end{aligned}$$

- The third Revan entropy

$$\begin{aligned} \mathcal{E}_{\eta R_3(M)} &= \log(\eta R_3(M)) - \frac{1}{\eta R_3(M)} \\ &\quad \log\left[\prod_{xy \in W(M)} (\kappa(x) - \kappa(y))^{\binom{\kappa(x) - \kappa(y)}{\kappa(x) - \kappa(y)}}\right] \\ \mathcal{E}_{\eta R_3(M)} &= \log(16p) - \frac{\log(2 \times (2)^2)}{16p} - \frac{\log(2 \times (0)^0)}{16p} \\ &\quad - \frac{\log(4(4p - 1) \times (1)^1)}{16p} - \frac{\log((4p(3p - 2) + 1) \times (0)^0)}{16p} \end{aligned}$$

- The first Revan vertex entropy

$$\mathcal{E}_{\mathcal{R}_1(M)} = \log(\mathcal{R}_1(M)) - \frac{1}{\mathcal{R}_1(M)}$$

$$\log\left[\prod_{xy \in W(M)} ((r(\bar{x}))^2)^{(r(\bar{x}))^2)}\right]$$

$$\mathcal{E}_{\mathcal{R}_1(M)} = \log(8p^2 + 32p + 18) - \frac{\log(2 \times (9)^9)}{8p^2 + 32p + 18}$$

$$- \frac{\log(8p \times (4)^4)}{8p^2 + 32p + 18} - \frac{\log(8p^2 \times (1)^1)}{8p^2 + 32p + 18}$$

Upon assessing Table 5 and Figure 3, it becomes clear that the expansion rate of the $\mathcal{E}_{\mathcal{B}_1(M)}$ index and the $\mathcal{E}_{\mathcal{B}_2(M)}$ index shows almost same growth as p increases. Similarly, it is noticeable that when the value of p increases, the growth rate of the $\mathcal{E}_{\mathcal{H}\mathcal{B}_2(M)}$ index surpasses that of $\mathcal{E}_{\mathcal{H}\mathcal{B}_1(M)}$.

Table 5. Entropy of K -Banhatti and Revan indices of MgO(111).

p	$\mathcal{E}_{\mathcal{B}_1(M)}$	$\mathcal{E}_{\mathcal{B}_2(M)}$	$\mathcal{E}_{\mathcal{H}\mathcal{B}_1(M)}$	$\mathcal{E}_{\mathcal{H}\mathcal{B}_2(M)}$	$\mathcal{E}_{\mathcal{H}_b(M)}$	$\mathcal{E}_{\eta\mathcal{R}_1(M)}$	$\mathcal{E}_{\eta\mathcal{R}_2(M)}$	$\mathcal{E}_{\eta\mathcal{R}_3(M)}$	$\mathcal{E}_{\mathcal{R}_1(M)}$
1	5.019	5.616	6.655	7.181	2.442	4.634	3.904	2.343	3.540
2	6.556	7.062	8.383	9.276	3.595	5.831	4.873	3.165	4.453
3	7.379	7.881	9.251	10.218	4.334	6.530	5.484	3.642	5.045
4	7.951	8.457	9.843	10.842	4.870	7.02	5.933	3.972	5.487
5	8.392	8.902	10.295	11.311	5.290	7.42	6.289	4.223	5.842
6	8.752	9.265	10.662	11.689	5.636	7.744	6.586	4.426	6.139
7	9.056	9.571	10.971	12.006	5.930	8.020	6.841	4.595	6.395
8	9.319	9.837	11.238	12.279	6.185	8.262	7.065	4.741	6.620
9	9.552	10.071	11.474	12.519	6.412	8.476	7.265	4.868	6.822
10	9.760	10.281	11.684	12.733	6.615	8.670	7.446	4.982	7.004

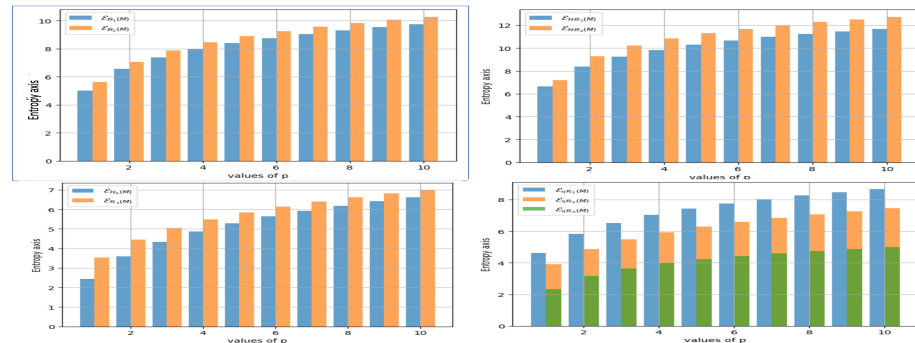


Figure 3. Graphical Representation of Entropy of Bhanhatti and Revan Indices.

Moving on, it can be observed that as p increases, the $\mathcal{E}_{\mathcal{H}_b(M)}$ index grows far faster than $\mathcal{E}_{\mathcal{R}_1(M)}$. Similarly, the $\mathcal{E}_{\eta\mathcal{R}_1(M)}$ index grows faster than the $\mathcal{E}_{\eta\mathcal{R}_2(M)}$ and $\mathcal{E}_{\eta\mathcal{R}_3(M)}$ indices as p increases. $\mathcal{E}_{\eta\mathcal{R}_3(M)}$ shows a very steady increase.

This section explores the correlation between K -Banhatti and Revan indices and the corresponding entropy values. Academic researchers heavily depend on graphical and computational representations of their findings to optimize efficiency and reduce the need for costly laboratory procedures. The current investigation employed a particular research methodology to analyze the correlation between the advancement of entropy and many other variables. Linear regression is employed to assess the relationship between entropy and the indices. This methodology entailed the manipulation of fundamental factors. The analysis’s performance was evaluated using the RMSE. The simulations were performed utilizing Microsoft Excel software. The coefficients are displayed in Table 6.

Table 6. Linear Regression Analysis of Entropy of K-Banhatti and Revan indices of MgO(111).

$\mathcal{E}_{\mathcal{I}(M)}$	a	b	RMSE
$\mathcal{E}_{B_1(M)}$	1.43	12.40	1.11
$\mathcal{E}_{B_2(M)}$	1.43	12.94	1.11
$\mathcal{E}_{HB_1(M)}$	1.44	14.34	1.12
$\mathcal{E}_{HB_2(M)}$	1.45	15.40	1.15
$\mathcal{E}_{H_b(M)}$	1.41	9.24	1.07
$\mathcal{E}_{\eta R_1(M)}$	1.38	11.23	1.03
$\mathcal{E}_{\eta R_2(M)}$	1.34	9.92	0.96
$\mathcal{E}_{\eta R_3(M)}$	0.86	6.36	0.443
$\mathcal{E}_{R_1(M)}$	1.34	9.50	0.97

5. Conclusions

We calculated the K-Banhatti indices in this article. We derived analytical formulas by generalizing the K-Banhatti topological descriptors of MgO(111). Subsequently, we utilize our results in entropy equations to determine the entropies of K-Banhatti indices of MgO(111). The transition state of MgO(111) undergoes a significant rise as the p increases, resulting in the most substantial modification in entropy. This research employed linear regression to evaluate the relationship between entropy and the K-Banhatti index. To evaluate the precision of our findings, we utilized statistical metrics such as RMSE. Based on the findings of the analysis carried out, it has been seen that the third Revan index constantly yields the most favorable and progressively improving results. This may be attributed to its higher accuracy regarding the root mean square error (RMSE). The results were reported in both numerical and graphical formats. If the experimental values of the physical properties of MgO(111) are known, it is easy to verify which one of these indices is better for predicting the corresponding physical properties of MgO(111).

Author Contributions: N.A.: methodology, validation, investigation, writing original draft preparation, writing review and editing, H.T.: conceptualization, methodology, validation, investigation, writing original draft preparation, writing review and editing, project administration. All authors have read and agreed to the published version of the manuscript.

Funding: Norah Almalki has been supported by Taif University, Saudi Arabia.

Institutional Review Board Statement: Not applicable.

Informed Consent Statement: Not applicable.

Data Availability Statement: Data are contained within the article.

Conflicts of Interest: The authors declare no conflict of interest.

References

- Acharjee, M.; Bora, B.; Dunbar, R.I.M. On M-Polynomials of Dunbar Graphs in Social Networks. *Symmetry* **2020**, *12*, 932. [[CrossRef](#)]
- Baig, A.Q.; Imran, M.; Khalid, W.; Naeem, W. Molecular description of carbon graphite and crystal cubic carbon structures. *Can. J. Chem.* **2017**, *95*, 831–837. [[CrossRef](#)]
- Chu, D.; Ali, H.; Ali, D.A.; Nadeem, M.; Kirmani, S.A.K.; Ali, P. Comparative Study of Planar Octahedron Molecular Structure via Eccentric Invariants. *Molecules* **2023**, *28*, 556. [[CrossRef](#)]
- Mu, A.R.; Lobanov, L.; Karelson, V.S.M. Correlation of boiling points with molecular structure. 1. A training set of 298 diverse organics and a test set of 9 simple inorganics. *J. Phys. Chem.* **1996**, *100*, 10400–10407.
- Jain, A.R.; Lomaka, R.; Petrukhin, A.; Maran, R.; Karelson, U. Perspective on the relationship between melting points and chemical structure. *Cryst. Growth Des.* **2001**, *1*, 261–265.
- Wiener, H. Structural determination of paraffin boiling points. *J. Am. Chem. Soc.* **1947**, *69*, 17–20. [[CrossRef](#)]
- Perigidad, S.; Jamagoud, D.; Maled, S.; Gavade, Y. QSPR analysis of certain degree based topological indices. *J. Stat. Appl. Probab.* **2017**, *6*, 361–371.
- Ahmad, I.; Chaudhry, M.A.; Hussain, M.; Mahmood, T. Topological Descriptors on Some Families of Graphs. *J. Chem.* **2021**, *2021*, 6018893. [[CrossRef](#)]
- Kirmani, S.A.K.; Ali, P.; Azam, F. Topological indices and QSPR/QSAR analysis of some antiviral drugs being investigated for the treatment of COVID-19 patients. *Int. J. Quantum Chem.* **2021**, *121*, e26594. [[CrossRef](#)]

10. Hosseini, H.; Shafiei, F. Quantitative structure-property relationship models for the prediction of gas heat capacity of benzene derivatives using topological indices. *Match Commun. Math. Comput. Chem.* **2016**, *75*, 583–592.
11. Manzoor, S.; Siddiqui, M.K.; Ahmad, S.; Fufa, S.A. On computation of entropy measures and molecular descriptors for isomeric natural polymers. *J. Math.* **2022**, *2022*, 5219139. [[CrossRef](#)]
12. Ghani, M.U.; Campena, F.J.H.; Maqbool, M.K.; Liu, J.B.; Dehraj, S.; Cancan, M.; Alharbi, F.M. Entropy Related to K-Banhatti Indices via Valency Based on the Presence of C₆H₆ in Various Molecules. *Molecules* **2023**, *28*, 452. [[CrossRef](#)]
13. Kulli, V.R. New K-Banhatti Topological Indices. *Int. J. Fuzzy Math. Arch.* **2017**, *12*, 29–37. [[CrossRef](#)]
14. Kulli, V. On K Banhatti indices of graphs. *J. Comput. Math. Sci.* **2016**, *19*, 1–6.
15. Kulli, V.; Chaluvvaraju, B. Zagreb-k-banhatti index of a graph. *J. Ultra Sci. Phys. Sci. Sect. A* **2020**, *32*, 29–36. [[CrossRef](#)]
16. Naz, K.; Ahmad, S.; Siddiqui, M.K.; Bilal, H.M.; Imran, M. On Some Bounds of Multiplicative K Banhatti Indices for Polycyclic Random Chains. *Polycycl. Aromat. Compd.* **2023**, 1–22. [[CrossRef](#)]
17. Hussain, M.; Siddiqui, M.K.; Hanif, M.F.; Mahmood, H.; Saddique, Z.; Fufa, S.A. On K-Banhatti indices and entropy measure for rhodium (III) chloride via linear regression models. *Heliyon* **2023**, *9*, e20935. [[CrossRef](#)]
18. Nasir, S.; Farooq, F.B.; Idrees, N.; Saif, M.J.; Saeed, F. Topological characterization of nanosheet covered by C₃ and C₆. *Processes* **2019**, *7*, 462. [[CrossRef](#)]
19. Zhao, Q.; Li, F.; Huang, C. Phosphorescent heavy-metal complexes for organic light-emitting diodes. *Chem. Soc. Rev.* **2010**, *39*, 3007–3030. [[CrossRef](#)]
20. Zhu, K.; Hu, J.; Kuebel, C.; Richards, R. Efficient preparation and catalytic activity of MgO (111) nanosheets. *Angew. Chem. Int. Ed.* **2006**, *45*, 7277–7281. [[CrossRef](#)]
21. Goniakowski, J.; Noguera, C.; Giordano, L. Using polarity for engineering oxide nanostructures: structural phase diagram in free and supported MgO (111) ultrathin films. *Phys. Rev. Lett.* **2004**, *93*, 215702. [[CrossRef](#)] [[PubMed](#)]
22. Jahanbani, A. On topological indices of carbon nanocones and nanotori. *Int. J. Quantum Chem.* **2019**, *119*, e26082. [[CrossRef](#)]
23. Selvamani, T.; Sinhamahapatra, A.; Bhattacharjya, D.; Mukhopadhyay, I. Rectangular MgO microsheets with strong catalytic activity. *Mater. Chem. Phys.* **2011**, *129*, 853–861. [[CrossRef](#)]
24. Imran, M.; Siddiqui, M.K.; Abunamous, A.A.E.; Adi, D.; Rafique, S.H.; Baig, A.Q. Eccentricity-Based Topological Indices of an Oxide Network. *Mathematics* **2018**, *6*, 126. [[CrossRef](#)]
25. Kulli, V.R. On K hyper-Banhatti indices and coindices of graphs. *Int. Res. Pure Algebr.* **2016**, *6*, 300–304.
26. Kulli, V.R. Harmonic Zagreb-K-Banhatti index of a graph. *Int. J. Math. Trends Technol.* **2020**, *66*, 123–132.

Disclaimer/Publisher’s Note: The statements, opinions and data contained in all publications are solely those of the individual author(s) and contributor(s) and not of MDPI and/or the editor(s). MDPI and/or the editor(s) disclaim responsibility for any injury to people or property resulting from any ideas, methods, instructions or products referred to in the content.